

# Transpolarizing Surfaces and Potential Applications

Pere J. Ferrer<sup>1</sup>, José M. González-Arbesú<sup>1</sup>, Christophe Craeye<sup>2</sup>, and Jordi Romeu<sup>1</sup>

<sup>1</sup> *AntennaLab - TSC, Universitat Politècnica de Catalunya (UPC)  
c/ Jordi Girona, 1-3, D3-212, 08034 Barcelona, Spain*

E-mail: pj.ferrer@tsc.upc.edu

<sup>2</sup> *Laboratoire TÉLÉ, Université catholique de Louvain (UCL)  
Place de Levant, 2, B-1348 Louvain-la-Neuve, Belgique*

**Abstract**— Transpolarizing surfaces are characterized for their property of rotating by 90° the reflected electric field with respect to the incident one. Several transpolarizing surface designs are presented, and their potential applications and limitations, mostly for oblique incidence, are discussed.

## I. INTRODUCTION

Transpolarizing surfaces are basically reflector devices that can easily rotate the polarization plane of an incident wave by 90°. Such surfaces are also referred as cross-polarizing surfaces or twist polarizers. Typical transpolarizing surfaces are composed of a unidirectional periodic metallic gratings (grids, strips or corrugations), approximately a quarter wavelength ( $\lambda/4$ ) above a metallic ground plane [1]-[3]. A sketch of the principle of operation of a simple transpolarizing surface is shown in Fig. 1. An incident electric field  $E_{inc}$  linearly polarized and oriented 45° with respect to the strips can be decomposed into two components:  $E_{\parallel}$  (parallel to the strips) and  $E_{\perp}$  (orthogonal to the strips). The  $E_{\parallel}$  is reflected with a phase of 180°, reversing the electric field component, because the strips behave like a perfect electric conductor (PEC). On the other hand, the  $E_{\perp}$  is reflected with a phase of 0°, because the combination of strips and gaps above a backing ground plane behaves like an artificial magnetic conductor (AMC). So, taking into account both effects, the reflected electric field  $E_r$  is rotated by 90° with respect to the incident electric field  $E_{inc}$ . Thus, many applications would arise from the polarization conversion property of such surfaces.

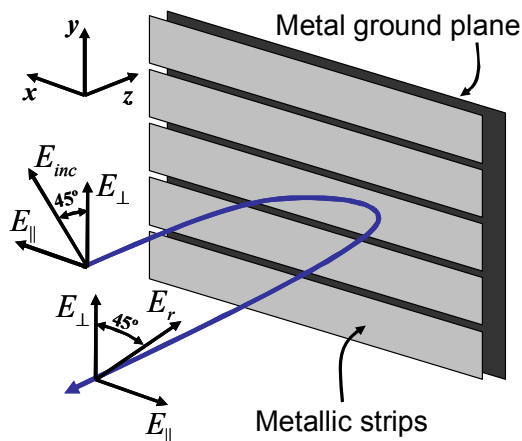


Fig. 1 Basic principle of operation of a transpolarizing surface.

However, transpolarizing surface designs could present other geometries different from the periodic arrangement of strips or corrugations. In this way, when a plane wave impinges on an array of square metallic patches above a ground plane, the phase of the reflected electric field is 0° at the resonance, behaving as an AMC, whereas its magnitude remains ideally close to 1 V/m (or 0 dB). The same result for normal incidence is expected when adding metallic vias to the previous surface, connecting the square patches to the ground plane, producing the so called electromagnetic band-gap (EBG) surface [4]. But if an offset vias is used instead [5], not the phase but the magnitude of the reflected copolar component can be decreased, at the same time as the cross-polar component is increased around the frequency of operation, showing a transpolarizing behaviour. Finally, another transpolarizing design composed of metallic square patches with a diagonal slot above a metal ground plane was presented as a broadband transpolarizing surface without the use of vias [6]-[7].

Notice the important role of the asymmetry between the incident electric field and the direction of the periodic gratings. Most transpolarizing surfaces are usually made using planar technology, although the corrugations and vias are not always easy to implement. Moreover, the transpolarizing effect is fairly achieved for normal incidence, but the results for oblique incidence are not obvious.

The potential applications of the transpolarizing surfaces will be discussed in the following sections, as well as, the simulation, fabrication and measurement processes for the realization of a transpolarizing surface following the design guidelines presented in [6]-[7].

## II. POTENTIAL APPLICATIONS

Since the principle of operation of the transpolarizing surfaces imply the decrease of the reflected copolar component and the increase of the cross-polar one, most applications of such surfaces will be devoted to the polarization conversion.

### A. Polarization conversion surface

Transpolarizing surface designs typically convert from the copolar component or polarization ( $E_x$ ) to the cross-polar one ( $E_y$ ) at the frequency of operation. This corresponds to a linear-to-linear polarization conversion. This property has been applied to reduce the blockage effect of a subreflector in Cassegrain antenna systems [1], [3] and [8].

Another application of the linear-to-linear transpolarization property, is that the incident circular polarized electric field is reflected preserving its handedness [5]-[7], contrary to the response of a typical metallic surface. This feature can be applied to generate a circularly polarized wave from a linearly polarized one, when placing a dipole antenna oriented along the 45° direction above an artificial ground plane composed of rectangular patches with a backing ground plane [9]-[10].

### B. RCS reduction

For single polarization radar systems, the polarization conversion property can be used to reduce the RCS of a target. By using a transpolarizing surface [6]-[7] as a cover, a decrease of more than 20 dB can be achieved for the copolar component.

### C. Polarimetric radar calibration

The third application of the transpolarizing surfaces concerns their use in calibration targets for polarimetric radar applications. It is well known that trihedral corner reflectors are often used for calibrating purposes although they can not provide a cross-polar response. Many designs can be found in the literature, showing a transpolarizing surface composed of diagonal corrugations or grids on one side of the trihedral corner reflector [11]-[12]. The designs comprising corrugations are heavy, and they need a minimum thickness of about  $\lambda/4$ . A thinner design made with the help of the transpolarizing surface design from [6]-[7] applied to a dielectric substrate with a thickness of about  $\lambda/20$  at the frequency of operation was proposed in [13] to produce a trihedral corner reflector with cross-polar response.

## III. DESIGN OF A TRANSPOLARIZING SURFACE

According to [6]-[7], a transpolarizing surface is composed of a periodic arrangement of metallic square patches with a wide diagonal slot in the centre of each patch, above a conducting ground plane. A finite element method (FEM), the well known Ansoft's HFSS [14], has been used to carry out the simulations. But due to memory and computing time limitations, such surfaces should be analysed by means of a single unit cell where periodic boundary conditions will be applied to simulate an infinite array approach. A sketch of a unit cell is depicted in Fig. 2.

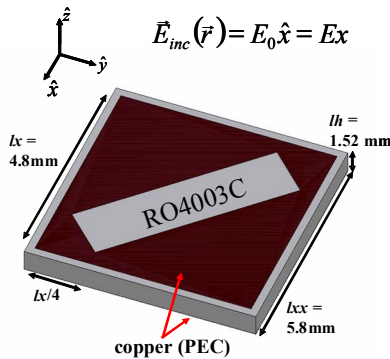


Fig. 2 Sketch of a unit cell comprising the square patch with a diagonal slot on one side of the substrate and a ground plane on the other side.

The square patch width ( $l_x$ ) is 4.8 mm, and the unit cell width ( $l_{xx}$ ) is 5.8 mm, with a gap of 1 mm ( $l_g$ ) between adjacent patches. The diagonal slot starts at 0.25 mm from the edge of the patch and  $l_x/4$  from its corner. Rogers RO4003C has been considered to simulate a real dielectric substrate with a thickness ( $l_h$ ) of 1.52 mm, and an electric permittivity ( $\epsilon_r$ ) of 3.32.

The simulated reflected results have been plotted in Fig. 3, for a linear incident electric field polarized along the  $x$  axis ( $E_x$ ). It can be seen that the magnitude of the  $E_x$  (copolar) component varies across the whole frequency band, having its minimum around 9.6 GHz. And it is remarkable how the  $E_y$  (cross-polar) component appears, having its maximum value around the frequency of interest, producing the polarization conversion. In this way, a 20 dB transpolarizing level has been achieved over a bandwidth of about 8% for normal incidence.

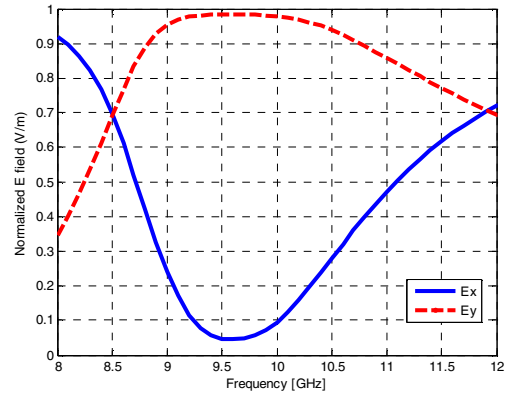


Fig. 3 Simulated reflected copolar ( $E_x$ ) and cross-polar ( $E_y$ ) components for normal incidence.

Simulations have also been carried out for a 45° oblique incidence; results can be seen in Fig. 4. Notice that the frequency of operation has been slightly shifted towards higher values, while the transpolarization level is also decreased, as compared to the normal incidence case.

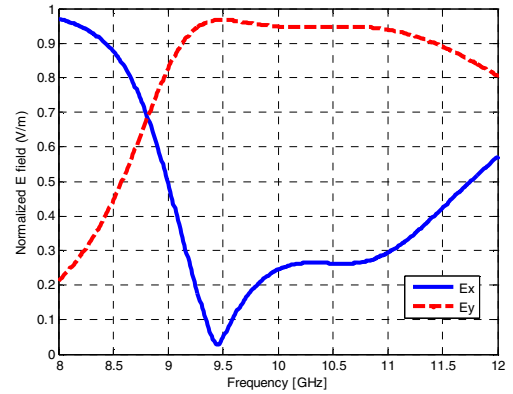


Fig. 4 Simulated reflected copolar ( $E_x$ ) and cross-polar ( $E_y$ ) components for 45° oblique incidence.

## IV. FABRICATION AND MEASUREMENTS

In order to verify the previously simulated results, a transpolarizing surface has been fabricated using standard

photo-etching techniques. The dimensions of the surface are  $150 \times 150 \text{ mm}^2$  ( $4.8\lambda \times 4.8\lambda$ ), and the thickness is  $1.52 \text{ mm}$  ( $\lambda/20$ ). A Rogers RO4003C substrate has been used as the dielectric substrate;  $26 \times 26$  unit cells (patches with slot) have been etched on one side of the substrate, whereas the opposite side remains as the metallic backing ground plane. The fabricated transpolarizing surface operating around  $9.6 \text{ GHz}$  can be seen in Fig. 5.

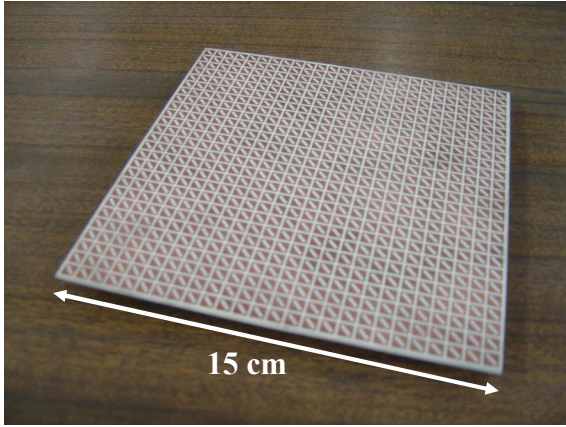


Fig. 5 Fabricated transpolarizing surface.

Bi-static RCS measurements have been carried out in the anechoic chamber. Two broadband ridged horns have been used in the measurements in two configurations: copolar (HH, VV) and cross-polar (HV, VH). The transpolarizing response has been measured with the help of a network vector analyser. Measured S-parameter results have been computed using a FFT conversion and windowing/gating at the surface position in the time domain, in order to avoid the strong mutual coupling between the two close ridged horn antennas. For this reason, the measured results slightly depend on the window type and on the window length, yielding higher or lower ripples in the processed results. The measured results for normal incidence can be seen in Fig. 6, showing a very good agreement the simulated ones, with a slight decrease in the transpolarization level at the operational frequency.

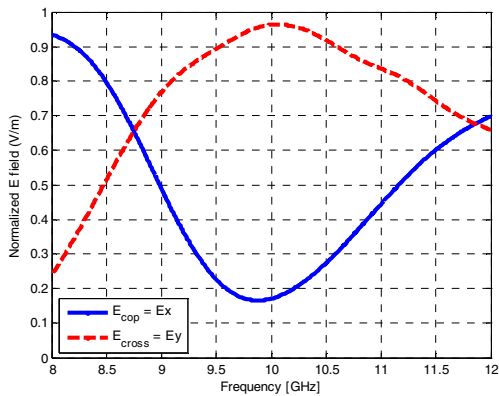


Fig. 6 Measured reflected copolar ( $E_x$ ) and cross-polar ( $E_y$ ) components for normal incidence.

Moreover,  $45^\circ$  oblique incidence measurements have been carried with the help of a dihedral corner reflector. It is well known that a dihedral corner provides a high level of copolar response, and consequently a low level of cross-polar response, for line of propagation perpendicular to the dihedral wedge. The results are complementary when the dihedral corner reflector is rotated by  $45^\circ$ . In this way, when putting the fabricated transpolarizing surface on one side of the dihedral, the results should be reversed.

Nevertheless, the measured results using the dihedral corner reflector and the transpolarizing design (not shown here), have not been as good as expected [13]. Many reasons appear to describe the low signal level in reception for both copolar and cross-polar results in the two positions of the dihedral ( $0^\circ$  and  $45^\circ$ ). It seems that for oblique incidence, some surface currents appear, producing a non-specular reflection, and hence, reducing the measured reflected field.

For this reason, the EBG principle [4] has been applied to our transpolarizing design. Adding vias which connect the square patch with the ground plane should reduce the surface currents, mostly when operating around the EBG region. Notice that the position of the vias is also critical, since an offset via can also produce the transpolarizing phenomenon [5]. So, the vias has been placed in one corner of the square patch, to minimize its effect on the transpolarizing behaviour introduced by the patch and the diagonal slot. After several optimizations, the new transpolarizing surface has been fabricated, as it can be seen in Fig. 7. The patch and slot dimensions are very similar to those of the previous design. The via diameter is  $0.6 \text{ mm}$ , and the fabrication procedure also involves a drilling process to produce the holes, and a metallization process to cover the holes by a thin metal layer, which connects the square patches (on one side of the substrate) and the ground plane (on the opposite side).

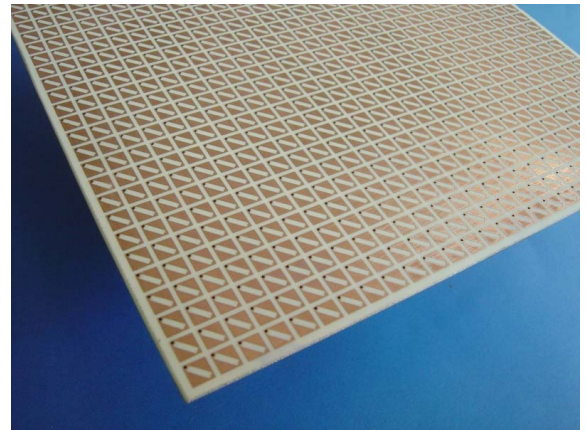


Fig. 7 Fabricated transpolarizing surface with the vias in one corner of the square patches.

Once fabricated, the transpolarizing surface with the vias has been measured in the anechoic chamber to assess the simulation results. The measured results for normal incidence have been plotted in Fig. 8. The transpolarizing response has

been found around 9.6 GHz, with a measured transpolarizing level of about 20 dB.

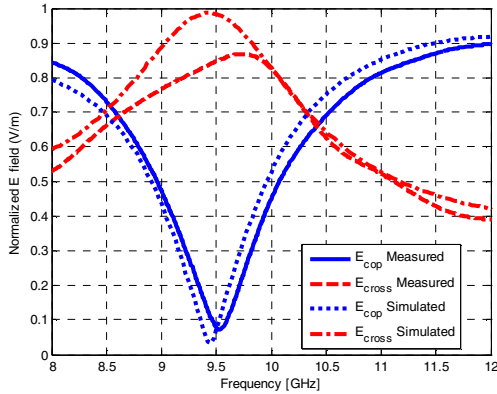


Fig. 8 Measured and simulated reflected copolar ( $E_x$ ) and cross-polar ( $E_y$ ) components for normal incidence of the transpolarizing surface with vias.

And the  $45^\circ$  oblique incidence measurements have been also carried out with the help of a dihedral corner reflector. One side of the dihedral is made of the transpolarizing surface with vias, and the measured results for a  $45^\circ$  orientation of the dihedral have been plotted in Fig. 9. For this orientation of the dihedral, a high cross-polar and, consequently, a low copolar levels are expected for the metallic dihedral. However, it can be seen from the measurement results that, when introducing the transpolarizing surface with vias on one side of the dihedral, the cross-polar level is decreased at the same time as the copolar level is increased, not as high as expected, but much better than the results with the transpolarizing surface without vias. Despite the insertion losses, a transpolarizing ratio of more than 12 dB has been achieved. These results show the important role of the metallic vias in the reduction of the surface waves for oblique incidence, and hence, the enhancement of the performance of such transpolarizing surfaces.

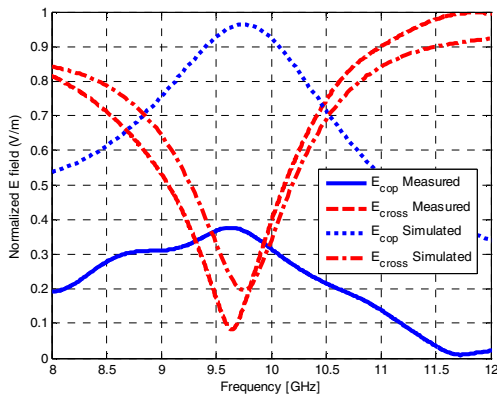


Fig. 9 Measured and simulated reflected copolar and cross-polar components for  $45^\circ$  oblique incidence of the transpolarizing surface with vias on one side of a dihedral corner reflector.

## V. CONCLUSIONS

Several transpolarizing surfaces have been presented. In such surfaces, the asymmetry of the gratings with respect to

the incident electric field (oriented at  $45^\circ$ ) plays an important role to produce the transpolarizing response. One transpolarizing surface has been designed and fabricated, achieving a very good agreement between the simulated and measured results for normal incidence. Oblique incidence has been measured indirectly with the help of a dihedral corner reflector, expecting a reversed Polarimetric response. The initial bad oblique incidence results have been improved with the introduction of metallic vias in the transpolarizing surface. A measured transpolarizing ratio of about 20 dB has been achieved for normal incidence, and about 12 dB for oblique incidence.

## ACKNOWLEDGMENT

This work has been partially supported by the Spanish Comisión Interministerial de Ciencia y Tecnología (CICYT) del Ministerio de Educación y Ciencia and FEDER funds through the grant TEC 2006-13248-C04-02/TCM, and by the European Commission through the METAMORPHOSE Network of Excellence Project FP6/NMP3-CT-2004-500252. In addition, the authors wish to thank Albert Aguasca, Rubén Tardío and Joaquim Giner for their valuable support in the fabrication of the transpolarizing surfaces.

## REFERENCES

- [1] D.S. Lerner, "A wave polarization converter for circular polarization", *IEEE Trans. Antennas Propag.*, vol. 13, no. 1, Jan. 1965.
- [2] J.D. Hanfling, G. Jerinic, L.R. Lewis, "Twist reflector design using E-type and H-type modes", *IEEE Trans. Antennas Propag.*, vol. 29, no. 4, July 1981.
- [3] R. Kastner, R. Mittra, "A spectral-iteration technique for analyzing a corrugated-surface twist polarizer for scanning reflector antennas", *IEEE Trans. Antennas Propag.*, vol. 30, no. 4, July 1982.
- [4] D.F. Sievenpiper, L. Zhang, R.F.J. Broas, "High-impedance electromagnetic surfaces with a forbidden frequency band," *IEEE Trans. MTT.*, vol. 47, pp.2059-2074, Nov. 1999.
- [5] Dunbao Yan, Qiang Gao, Chao Wang, Chang Zhu, Naichang Yuan, "A novel polarization convert surface based on artificial magnetic conductor", *Microwave Conference Proceedings, APMC, 2005.*
- [6] P.J. Ferrer, B. Kelem, C. Craeye, "Design of Broadband Transpolarizing Surfaces", *Microw. Opt. Tech. Letters*, vol. 48, no. 12, pp.2606-2611, Dec. 2006.
- [7] P.J. Ferrer, J.M. González-Arbesú, J. Romeu, C. Craeye, "Design and Fabrication of a Cross-polarising AMC Surface", *Proc. 2nd European Conference on Antennas and Propagation (Eucap 2007)*, Edinburgh (UK), Nov. 2007.
- [8] K.C. Hwang, "Optimisation of broadband twist reflector for Ku-band application", *Electr. Lett.*, vol. 44, no. 3, Jan. 2008.
- [9] Fan Yang, Yahya Rahmat-Samii, "A low profile single dipole antenna radiating circularly polarized waves", *IEEE Trans. Antennas Propag.*, vol. 59, no. 9, Sept. 2005.
- [10] V.F. Fusco, S.W. Simms, "Reflected circular polarisation conservation using textured surface", *IET Electronics Letters*, vol. 43, no.18, 2007.
- [11] D.G. Michelson, E.V. Jull, "A depolarizing calibration target for radar polarimetry", *Proc. IEEE International Geoscience and Remote Sensing Symposium (IGARSS 1990)*, May 1990.
- [12] A. Macikunas, S. Haykin, "Trihedral twist-grid polarimetric reflector", *IEE Proc.-F*, vol. 140, no. 4, Aug. 1993.
- [13] P.J. Ferrer, C. López-Martínez, X. Fàbregas, J.M. González-Arbesú, J. Romeu, A. Aguasca, C. Craeye, "Transpolarizing Surfaces for Polarimetric SAR Systems Calibration", *Proc. IEEE International Geoscience and Remote Sensing Symposium (IGARSS 2007)*, Barcelona (Spain), July 2007.
- [14] Ansoft's HFSS (FEM numerical method), [www.ansoft.com/hfss/](http://www.ansoft.com/hfss/)